The Weibel Instability in Collisionless Relativistic Shocks

Tanim Islam

University of Virginia

The Weibel instability[1], purely electromagnetic in nature, has been used to explain the strong magnetic fields believed to occur in the highly relativistic shocks of gamma ray burst afterglows[2]. We will go through a quick derivation of the important properties of the relativistic Weibel instability in the simplest case (no magnetic fields, no electric fields, no equilibrium currents), as well as give a physical description for the instability. The results will then be connected through numerical simulations and order of magnitude estimates of the highly collisionless GRB afterglow. Finally, we end with a "laundry list" of what I believe are the most significant issues in describing such a shock, which perhaps cannot be described by laminar flows or other such streamlines.

The Physical Systems Being Described

- Both the gamma-ray burst afterglow shock and the pulsar winds are describable by a relativistic to highly relativistic collisionless plasma with (assumed) small seed magnetic fields.
- Shown below are calculated results of the expected gamma factors of the shocks in several GRBs, taken from [3]. Here γ factors of corresponding material range from a few to a few hundred.

TABLE 3

LIMITS ON SELECTED BURSTS

GRB	f_1	α	$e_{max}/m_e c^2$	z	$\hat{\tau}$	Limit A	Limit B	Reference
Bursts with Very High Energy Photons								
910503	8.71	2.2	333	1	3.0×10^{12}	**340**	300	1
910601	0.5	2.8	9.8	1	1.8×10^{11}	72	**110**	2
910814	13.5	2.8	117	1	4.7×10^{12}	**200**	190	3
930131	1.95	2.0	1957	1	7.0×10^{11}	**420**	270	4
940217	0.36	2.5	6614	1	1.2×10^{11}	**340**	120	5
950425	1.62	1.93	235	1	6.0×10^{11}	**300**	280	6
990123	1.1	2.71	37	1.6	1.2×10^{12}	150	**180**	7
Bursts with Redshifts								
971214	0.35	2	1	3.42	2.6×10^{12}	192	**410**	8
	0.1	3	1	3.42	7.5×10^{11}	64	**160**	8
980703	0.08	2	1	0.966	2.7×10^{10}	69	**140**	8
	0.02	3	1	0.966	8.0×10^{9}	24	**56**	8
990510	0.1	2	1	1.62	1.2×10^{11}	98	**200**	8
	0.03	3	1	1.62	3.7×10^{10}	34	**79**	8
Unusual Bursts								
980425	0.04	2	1	0.0085	1.0×10^{4}	4.6	**6.4**	8
	0.01	3	1	0.0085	2.9×10^{3}	2.8	**3.8**	8
970417a	...	...	2×10^{6}	0.3	8.7×10^{8}	**170**[a]	...	8, 9

NOTES.—Limit A is defined as $\gamma_{min} = \hat{\tau}^{1/(2\alpha+2)}(e_{max}/m_e c^2)^{(\alpha-1)/(2\alpha+2)}(1+z)^{(\alpha-1)/(\alpha+1)}$. Limit B is defined as $\gamma_{min} = \hat{\tau}^{1/(\alpha+3)}(1+z)^{(\alpha-1)/(\alpha+3)}$. The larger of the two limits is reported in boldface.

[a] An alternative method was used to calculate this limit.

REFERENCES.—(1) Schneid et al. 1992; (2) Hanlon et al. 1994; (3) Kwok et al. 1993; (4) Sommer et al. 1994; (5) Hurley 1994; (6) Catelli, Dingus, & Schneid 1996; (7) Briggs et al. 1999; (8) http://cossc.gsfc.nasa.gov/batse; (9) Atkins et al. 2000.

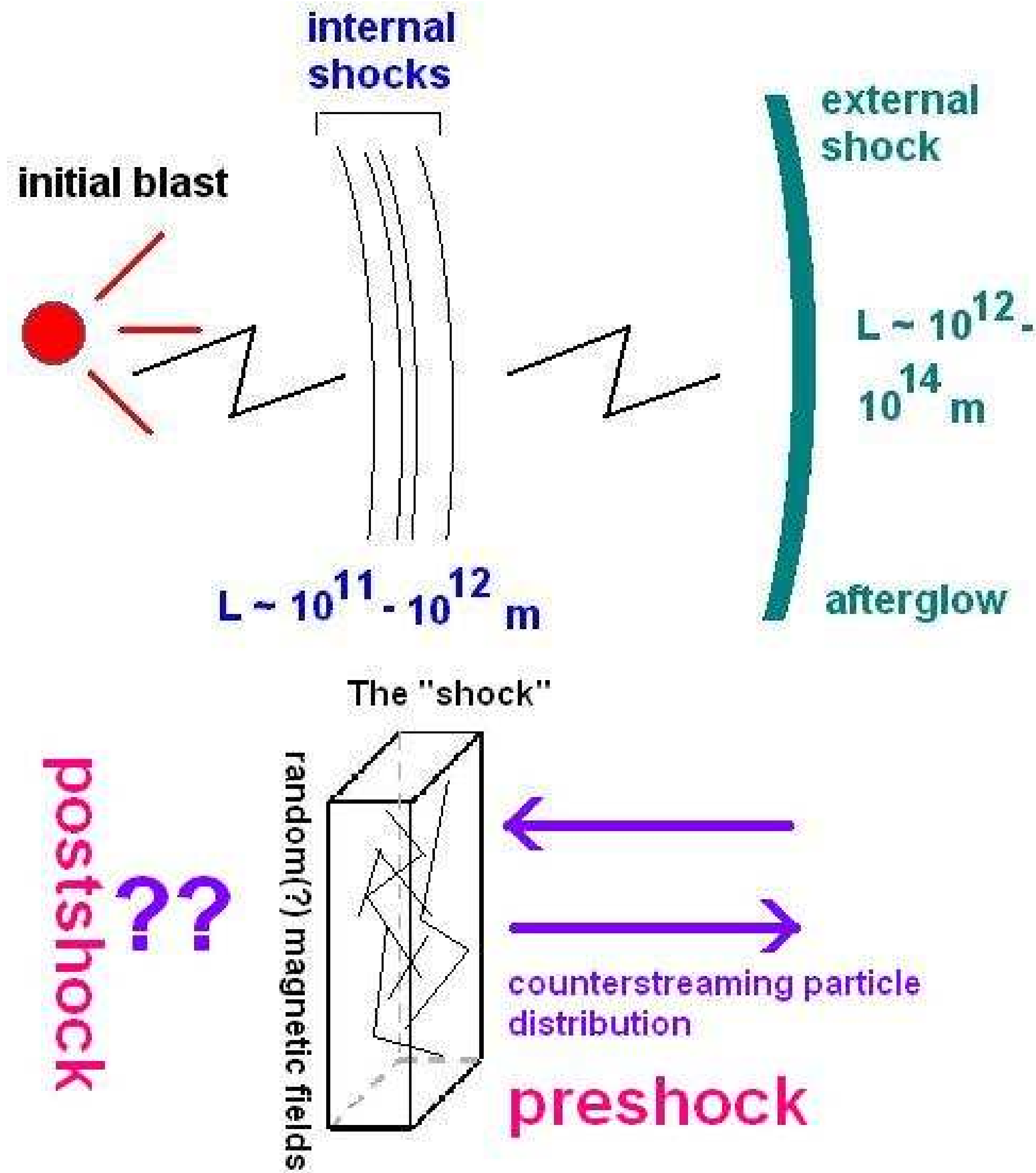

Very simplified model of the gamma ray burst with central enginem internal shocks, and external shocks. Also shown is the proposed mechanism that gives rise to the Weibel instability – initially some counterstreaming distribution in the preshock region.

Collisionless Approximation Valid

The relativistic plasma is also collisionless if we consider two-body collisions that result in the transfer of momentum or of energy.

- If we consider simply ion-ion collisions of the shock with the incoming preshock ISM plasma, with $\gamma_{\rm shock}$, then the timescale associated with collisional processes (i.e., magnetic diffusion from electrical resistivity, thermal diffusion and equilibration of the particle density function from collisional conductivity, momentum diffusion through viscosity) with the plasma incoming in the frame of the shock:

$$\tau_{\rm coll} \simeq 1/\nu_{\rm coll}$$

- For relativistic particles, the kinetic energy of particles $E = mc^2\gamma_{\rm shock} = e^2/r$. The cross section $\sigma \sim r^2$. The density of the shock is of order $n_{\rm ISM}\gamma_{\rm shock}$.
- One can show that $\nu_{\rm coll} \sim n\sigma c \simeq \left(e^2/mc^2\right)^2 \gamma_{\rm shock} n_{\rm ISM} c$.
- For values of typical ISM, $n_{\rm ISM} = 10^6$ m^{-3} and $\gamma_{\rm shock} = 100$, and taking the most conservative estimate (fastest collision rate):

$$\tau_{\rm coll} \simeq 4 \times 10^{12}\ {\rm s}$$

Much larger than associated lifetimes of afterglows (days, weeks, and sometimes months, but not thousands of years).

Justifications for the Weibel Instability

- It is a mechanism for the generation of (possibly) strong magnetic fields within the shock, on the order of up to a significant fraction of the total kinetic energy within the shock. Letting $\epsilon_B = B^2/(8\pi e_{\text{th}})$, the following groups have calculated from the afterglow spectra and the light curves the inverse plasma β:
  - $\epsilon_B \sim 0.1$[4, 5].
  - $\epsilon_B \sim 10^{-2}$[6].
  - $\epsilon_B \simeq 10^{-5}$[7, 8].
- The magnetic field strength due to Lorentz boosting of the ISM magnetic field, $B_{\text{shock}} \sim \gamma_{\text{shock}} B_{\text{ISM}}$, is many orders of magnitude too small to explain the spectra.
- The size of the progenitor maybe $\sim 10^5$ m. Afterglows appear at $\sim 10^{12}$ m, so flux freezing is insufficient to explain the magnetic fields as well; furthermore, the magnetized wind is also incapable of providing the large magnetic fields as well.
- Other effects: the acceleration of particles in the preshock region, due to magnetic field-particle interactions[9, 10, 11].
- Perhaps a characteristic scattering length given by the wavelength of the fastest-growing modes in this "tangled" magnetized plasma – this ℓ much smaller than mean free path of particles, so collisions via pitch-angle scattering[2] result in the use(?) of MHD approximation and the (!) Rankine-Hugoniot conditions.

The Weibel Instability in a Nutshell

- The *Weibel* instability is a purely *electromagnetic* (i.e., $\mathbf{E} = -c^{-1}\partial\mathbf{A}/\partial t$, where $\mathbf{A}$ is the vector potential) mode that converts an anisotropic particle distribution into magnetic energy.
- This mode can arise in the absence of equilibrium currents $\mathbf{J}$, in the absence of equilibrium electric and magnetic fields – as far as kinetic instabilities go, it is as "simple" as the expressions for Landau damping, electrostatic wave-particle resonances.
- Was first introduced by E. Weibel[1] in the context of then-weird instabilities seen in early plasma experiments.
- Has been applied to describe the anomalous resistivity in Earth's magnetosphere to efficiently drive magnetic reconnection (see, e.g., [12] and references therein).
- Weibel and other electromagnetic instabilities are dynamically important in intense laser-plasma interactions (see, e.g., [13] for some references).
- The general results for a nonisotropic, zero-current relativistic equilibrium were first explored by Yoon and Davidson[14] in describing the general stability properties.
- The maximum growth rate in the relativistic limit: $\gamma_{\max} \sim \gamma^{-1/2}\omega_p \rightarrow \lambda_{De}/c$, where $\omega_p^2 = 4\pi e^2/m$ is the plasma frequency and $\lambda_{De} = 4\pi e^2 c^2/E$ is the Debye length, and with wavenumber $k_{\max} \sim \gamma^{-1}\omega_p/c \rightarrow \lambda_{De}^{-1}$.

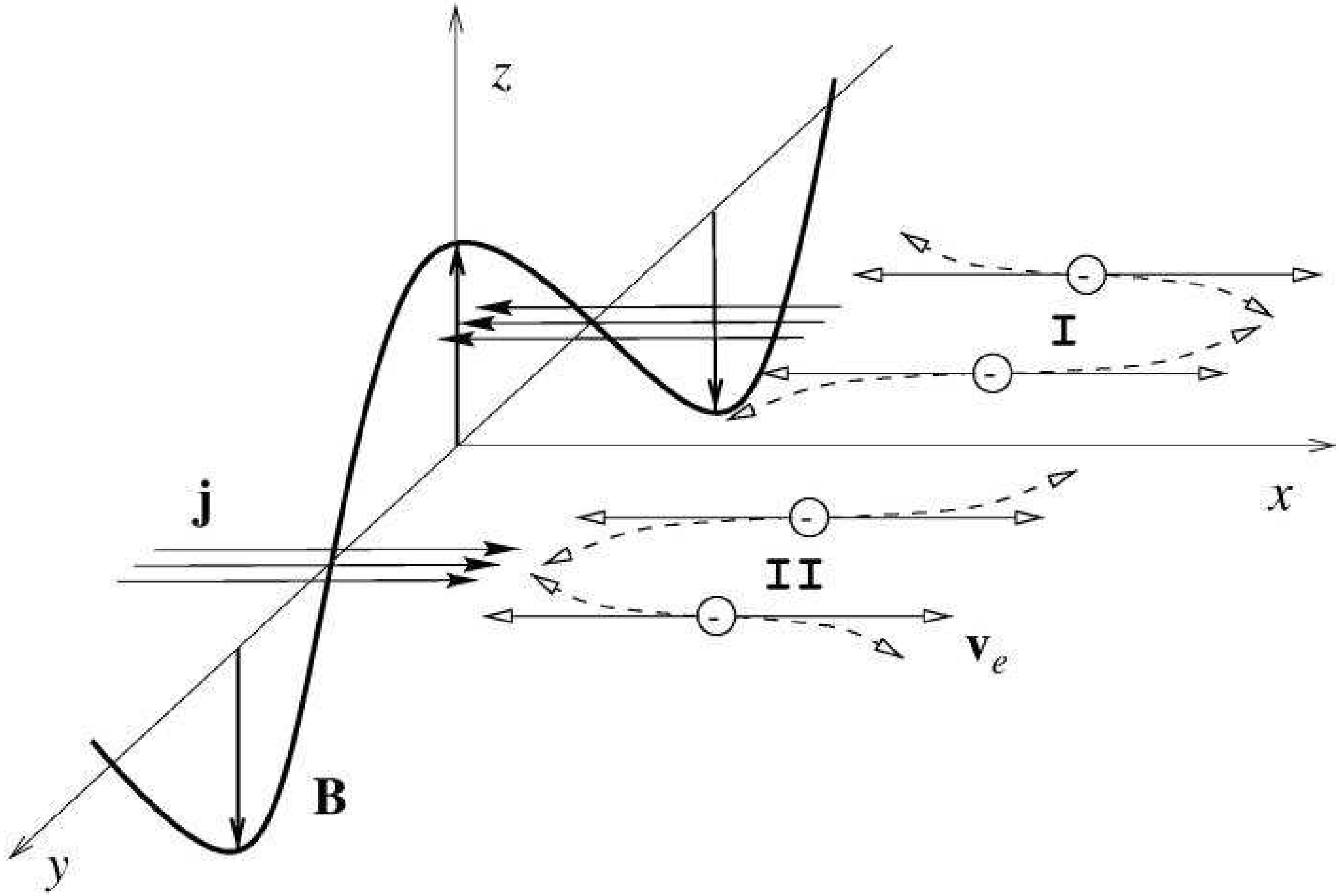

- A perturbation in the y axis creates magnetic fields in the z direction, which amplify the perturbation (and quench the anisotropy). This is also referred to as the *filamentation* instability, due to the establishment of current filaments in the nonlinear stage of this instability.

The Relativistic Weibel Instability in the Linear Regime

- Assume purely electromagnetic perturbations, so the vector potential is given by:

  $$\hat{\mathbf{A}} = \tilde{\mathbf{A}} \exp\left(i\mathbf{k}\cdot\mathbf{x} - i\omega t\right)$$

  So that electric and magnetic fields are given by:

  $$\hat{\mathbf{E}} = \frac{i\omega}{c}\hat{\mathbf{A}}$$
  $$\hat{\mathbf{B}} = i\mathbf{k}\times\hat{\mathbf{A}}$$

- Formally, for each group of particles with mass m_j, charge Z_j there is a total distribution function – sum of perturbed and equilibrium distributions:

  $$f_j = f_{0j} + \hat{f}_j$$

  And the collisionless Boltzmann equation for relativistic particle distributions:

  $$-i\left(\omega - \mathbf{k}\cdot\mathbf{x}\right)\hat{f}_j + iZ_je\left(-\frac{\omega}{c}\hat{\mathbf{A}} + \mathbf{v}\times\left(\mathbf{k}\times\hat{\mathbf{A}}\right)\right)\cdot\frac{\partial f_{0j}}{\partial\mathbf{p}} = 0$$

- Equations are closed by using Lorentz gauge $\mathbf{k}\cdot\hat{\mathbf{A}} = 0$ with this result:

  $$\left(k^2 - \omega^2/c^2\right)\hat{\mathbf{A}} = \frac{4\pi}{c}\mathbf{J} = \frac{4\pi}{c}\sum_j Z_je\int \mathbf{v}\hat{f}_j\, d^3\mathbf{v}$$

- Yoon and Davidson[14] used a simplistic particle distribution to find an analytic dispersion relation for the Weibel instability, as well as its stability criterion.

$$F\left(p_\perp^2, p_z\right) = \frac{1}{2\pi p_\perp}\delta\left(p_\perp - \hat{p}_\perp\right) \times \frac{1}{2\hat{p}_z} H\left(\hat{p}_z^2 - p_z^2\right)$$

What they find is the following important characteristic of the distribution – the associated $\hat{\gamma}$, $\hat{\beta}_z$, and $\hat{\beta}_\perp$:

$$\hat{\gamma} = \sqrt{1 + \frac{\hat{p}_\perp^2 + \hat{p}_z^2}{m^2 c^2}}$$
$$\hat{\beta}_z = \frac{\hat{p}_z}{\sqrt{\hat{p}_z^2 + m^2 c^2}}$$
$$\hat{\beta}_\perp = \frac{\hat{p}_\perp}{\sqrt{\hat{p}_\perp^2 + m^2 c^2}}$$

- They find that for a relativistic plasma $\gamma > 2$, the maximum growth rate is something that looks like c/λ_{De}, and hence the dominant wavenumber $k_{\max} \sim \lambda_{De}^{-1}$.

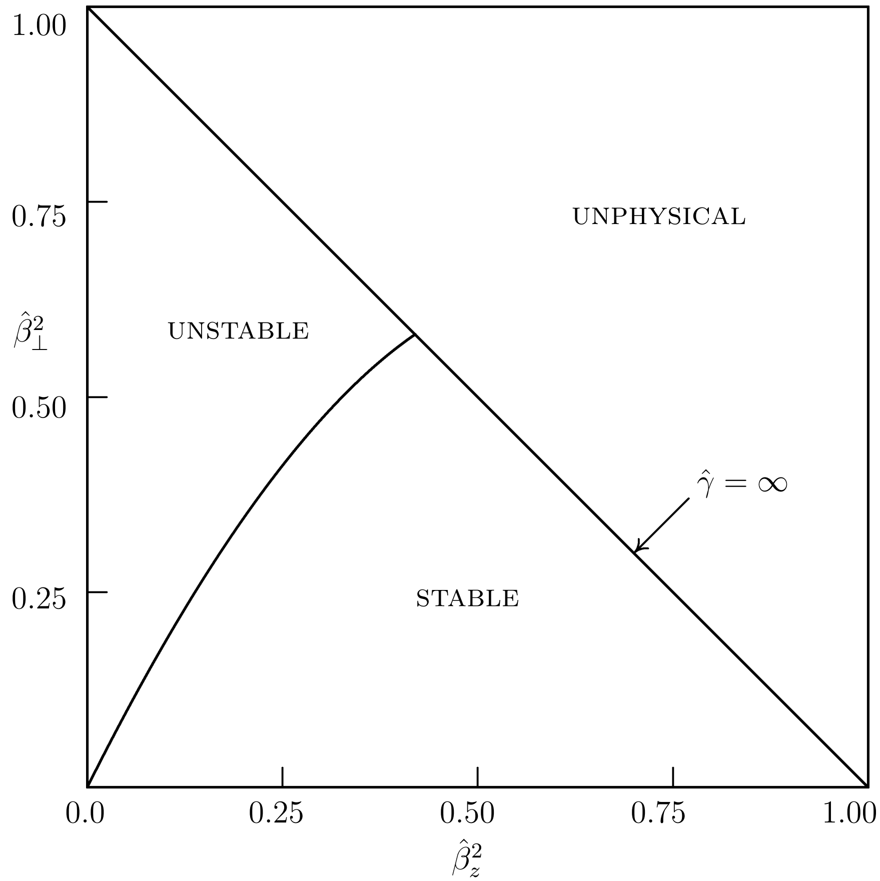

Visual depiction of stable, unstable, and unphysical regimes for the relativistic Weibel instability with an initial analytic momentum distribution.

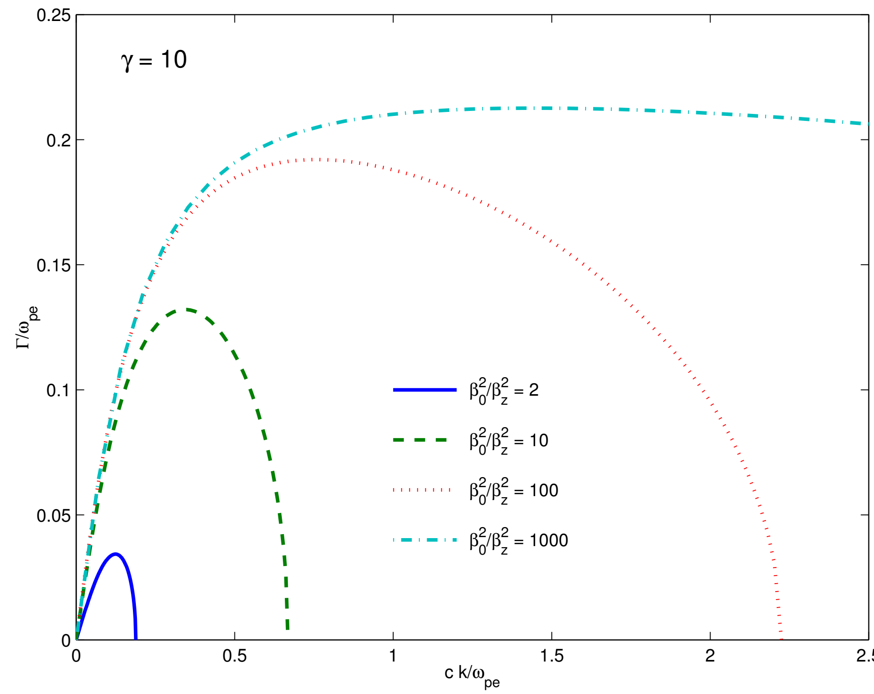

Plot of the growth rate for Weibel instability as a function of wavenumber k, for different ratios of $\hat{\beta}_\perp^2/\hat{\beta}_z^2$. Here, we have that $\hat{\gamma} = 10$.

Weibel Instability is NOT the Two-Stream Instability

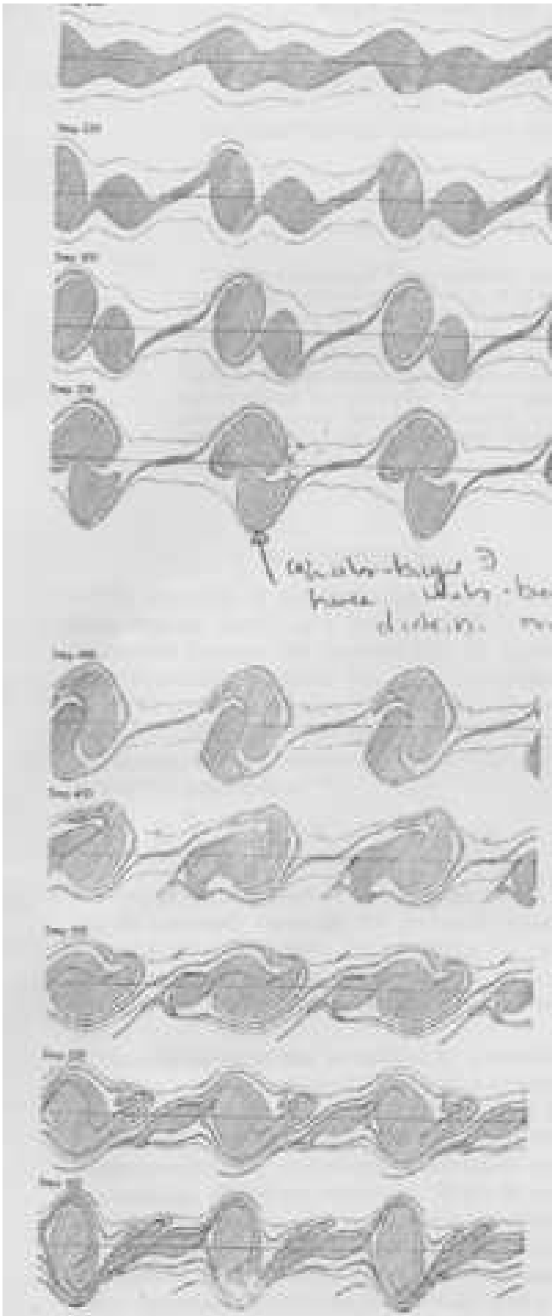

(b)

FIG. 5. The nonlinear development of a two-stream instability. The inner $F = 0$ region has been shaded to emphasize the development of hole structures.

The two-stream instability is characterized by a 3D system – one dimension of space (x), one dimension of velocity v_x, and one dimension of time. Therefore, since all currents $\mathbf{J} = J_x(x)\mathbf{e}_x$, this system is dimensionally constrained to be purely electrostatic. Shown on the left is the time evolution of the phase-space plot of the two interacting streams – horizontal is position, vertical is velocity, with the system being periodic in x.

General Results of the Weibel Instability from Numerical Simulations

- These models are typically PIC (particle in cell) codes with limited dimensionality – 2 spatial dimensions in space and velocity, to simulate at a minimum the evolution and existence of a magnetic field – in order to conserve computing power.
- Numerical studies of the Weibel instability in plasmas is usually done with electron-positron systems or systems in which the electrons move in a stationary ionic background (see, e.g., [13, 15]) that results in the saturation of the magnetic field, electron energy densities, etc. on time scales of order ω_{pe} in the nonrelativistic or mildly relativistic limit $\gamma \simeq 1$.
  - The large, saturated electric fields in the limit of electron saturation is expected to lead to the breakdown of ion stationarity – one must take into account ion dynamics on ion gyroperiods (calculated at roughly the electron saturation magnetic fields)[16].
  - In light of this important result, the model describing the GRB afterglow in terms of the electron and magnetic energy densities[17] *separately* may be flawed – in that these two quantities may be rather closely related.
- Magnetic fields saturate, depending on the nature of the counterstreaming (usually electron) beams, from anywhere near equipartition relative to electron energies, or somewhat below this

value – ***a problem that is still not well understood, and believed to be very complicated even in this limited regime***.

  – Even in regime where the electrons saturate (time scales smaller than ion gyroperiod), there exists a variety of, for example, particle-wave resonance effects (artifacts being the presence of velocity singularities in the particle distributions) and the excitation of electrostatic modes[18, 16], among other effects.

- Accelerations of particles cannot easily be described by Fermi acceleration across the shock (or the "active region" over which these instabilities operate) [10, 9].

- ***In all cases, at least in the electron saturation regime, kinetic numerical analysis shows the development of nonuniform particle distributions – not the simple thermalization of particle distributions.***

- Some full three-dimensional momentum and space PIC simulations of mildly relativistic counterstreams ($\Gamma = 5 - 10$) [10, 9] have just been started, but the results are not yet as comprehensively assayed as the simpler 2D models.

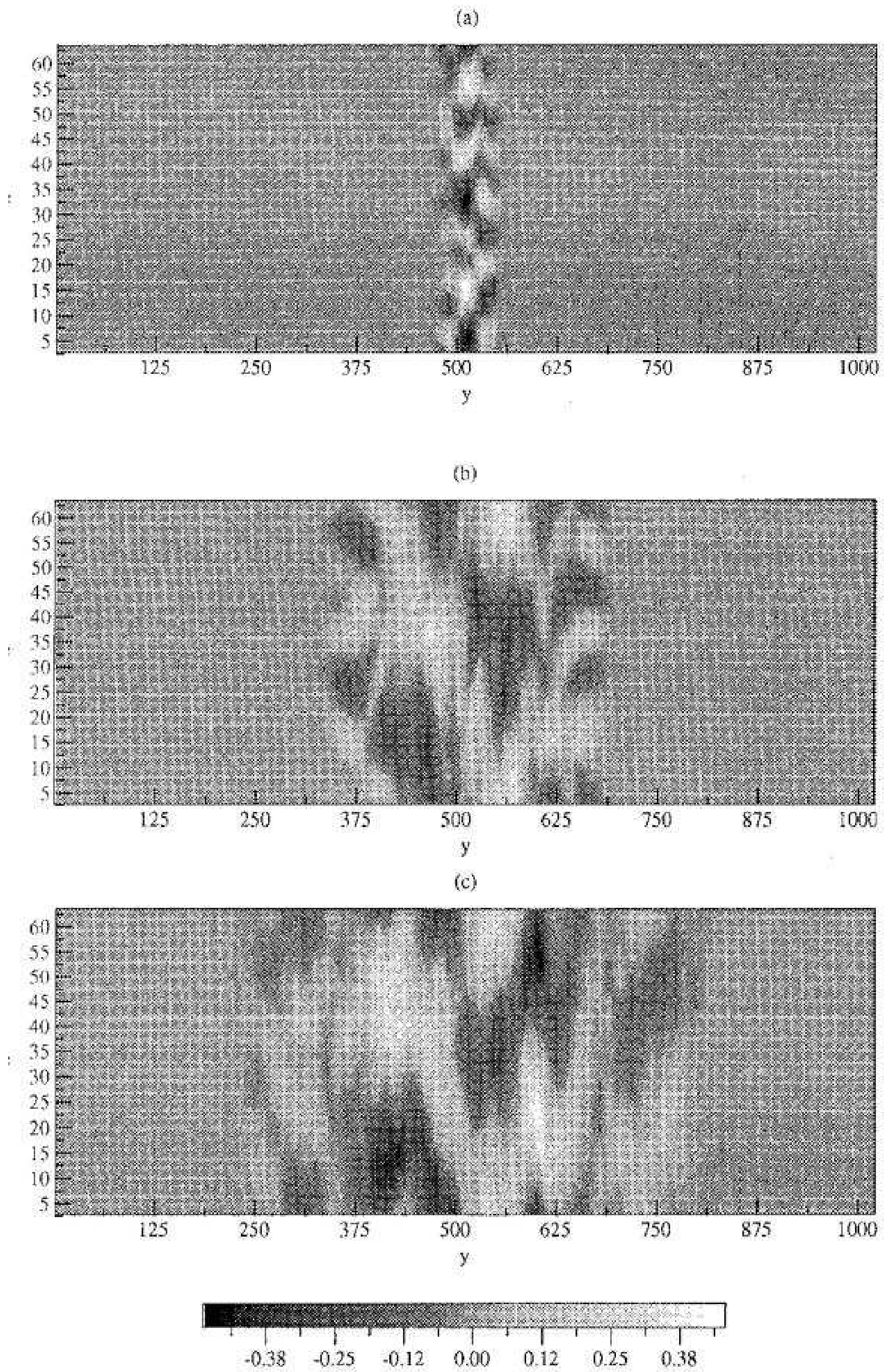

Characteristic filamentation structure of the magnetic field (and consequently, of the current and electron velocities) in the Weibel instability. In this problem, one has both mildly relativistic counterstreaming electron and positron plasmas, such as might be seen in pulsar winds[15].

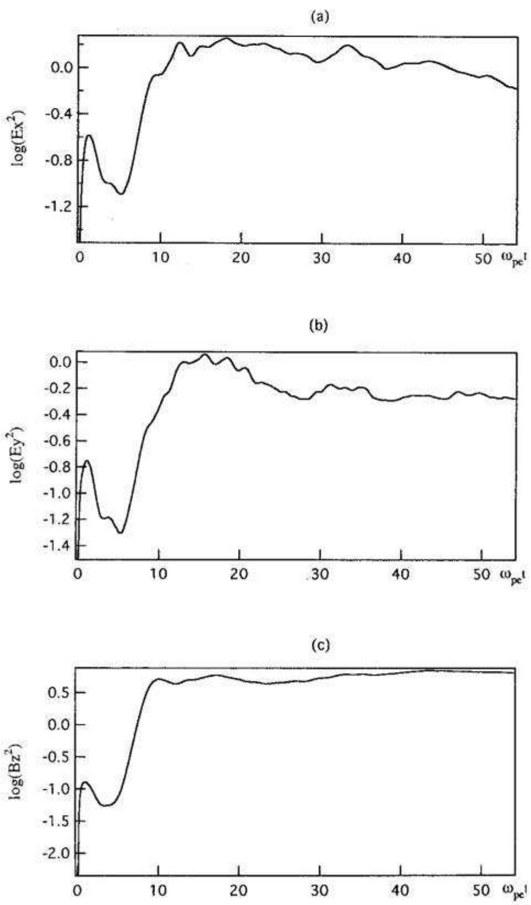

FIG. 3.—Time history of the electric field energy: (*a*) E_x^2, (*b*) E_y^2 and magnetic field energy, and (*c*) B_z^2, normalized by $2VtL_x/L_xL_y$, where V is the plasma front velocity of the streams, which is assumed to be constant.

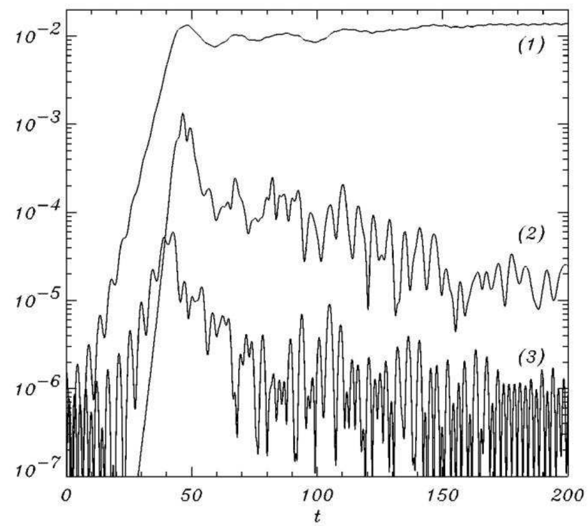

FIG. 1. The magnetic energy $\mathcal{B}$, curve 1, and the electric energies $\mathcal{E}_x$ and $\mathcal{E}_y$, curves 2 and 3, respectively, versus time for the asymmetric run.

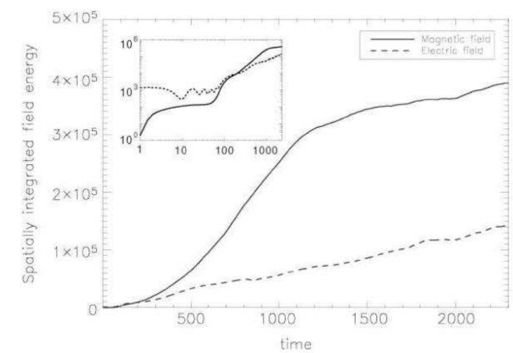

FIG. 5.— Total magnetic (full drawn) and electric (dashed) energy in the box as a function of time. The inset shows a log-log plot of the same data.

On the far left is shown the saturation of field quantities for the e^+e^- plasma[15]; in the middle is shown the saturation of an electron counterstreaming plasma's magnetic field energy density[16]; and on the right is showing the semisaturation of the magnetic field energy density (due to electron motion saturation) in the full 3 + 3 dimensional model of electron-ion plasma [11]. The first two models are truncated dimensionally in space and momentum. None of these models, however, takes into account the ion dynamics as well.

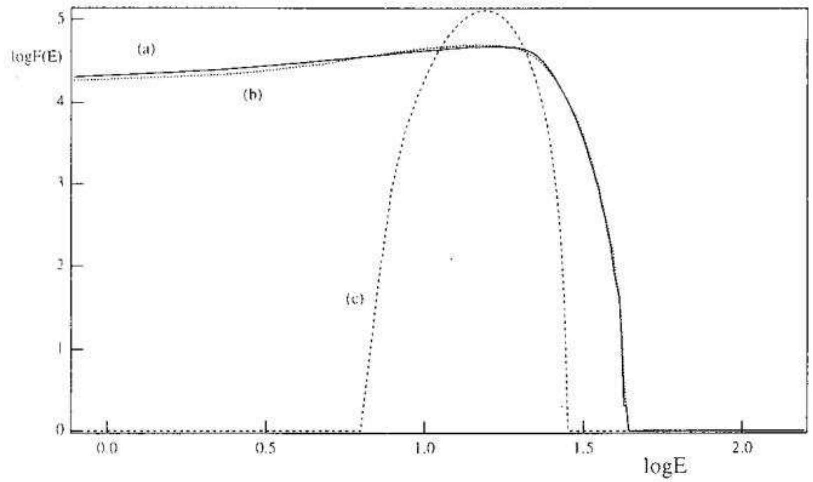

FIG. 4.—The (*a*) electron and (*b*) positron energy spectrum in the final state of the simulation. *E* normalized by the thermal energy is the total kinetic energy of particles. (*c*) The initial energy distribution of both particle species.

hfill

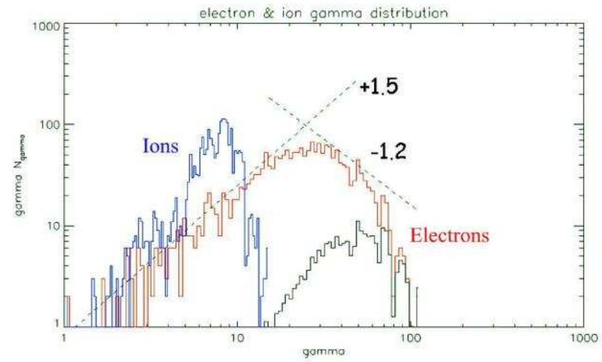

Figure 2: Probability Distribution Functions as produced by the collisionless shock in one of our experiments.

Highly nonthermal distributions for the positron-electron plasma (on left) and for the 3D electron plasma on the right. This is explained as particle acceleration in the plasma preshock[10] for the 3D plasma.

Additional Unusual Complexities Associated With the Weibel Instability

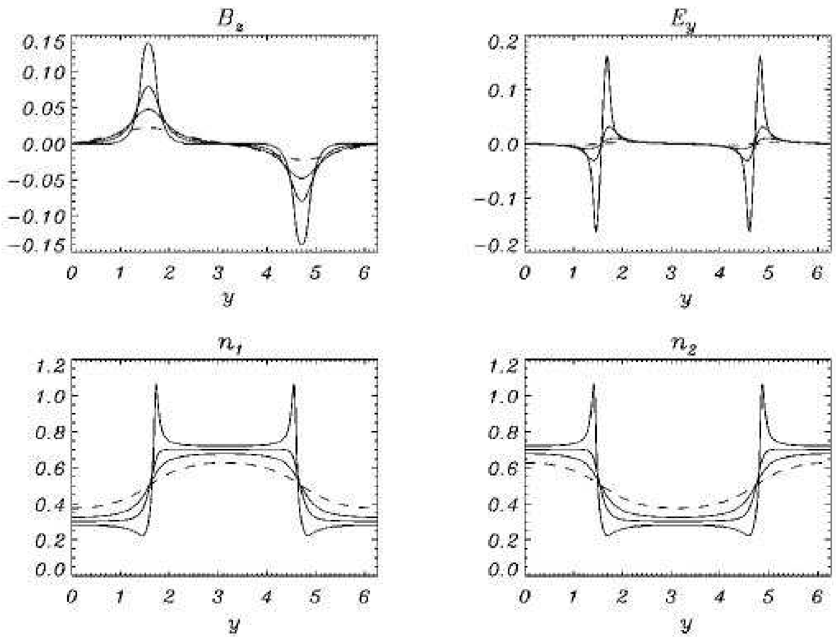

FIG. 4. The formation of the singularity in a symmetric case (run 1 in Table I). In the four frames we show the magnetic field, the y component of the electric field, and the densities of the two electron populations as a function of y at the end of the linear phase $t=60$ (dashed lines) and during the nonlinear evolution $t=70{,}72$ (solid lines).

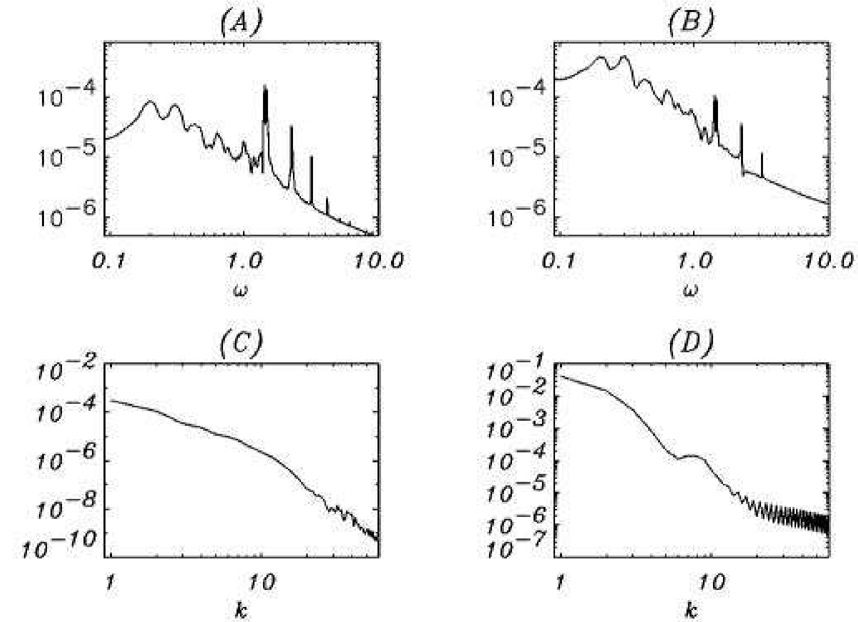

FIG. 9. The (squared) frequency spectrum of (A) B_z, (B) E_y during the nonlinear phase and the (squared) spatial spectrum of (C) B_z and (D) E_y at $t=180$.

On left is shown the singularities arising in the electron velocity distributions due to the Weibel instability – a wave-particle resonance effect. On the right, there is a characteristic frequency of oscillation as seen from a Fourier time spectrum map of the electric and magnetic fields.

Main Issues to be Resolved

- In the description of a "shock," no numerical model has imposed boundary conditions on the flow of momentum (both particle and electromagnetic), energy, and particles – very important if we are to describe this structure as a "shock."

- No numerical model of the Weibel instability has yet described a situation where the counterstream is ultrarelativistic; no one has yet done a full model taking into account the evolution of the ion particle distribution.

- The descriptions of a "turbulent" (or random) collection of magnetic fields in the absence of a strong background does not appear to make sense – how does one support an inherently random, non-force-free configuration with currents?

- The thermally ultrarelativistic plasma with ultrarelativistic counterstream seems an inherently less complicated problem – the effects of particle mass become irrelevant.

  - At sufficiently high particle energies, one may even ignore the effects of electromagnetic fields – one where $L < \lambda_{De}$, where L is the length scale of the problem and $\lambda_{De}^2 = 4\pi e^2 n/\bar{E}$, where $\bar{E}$ is the average particle energy.

References

[1] E. Weibel, Phys. Rev. Lett. **2**, 83 (1959).

[2] M. Medvedev and A. Loeb, Astrophys. J. **526**, 697 (1999).

[3] Y. Lithwick and R. Sari, Astrophys. J. **555**, 540 (2001).

[4] E. Waxman, Astrophys. J. **485**, L5 (1997).

[5] R. Wijers and T. Galama, Astrophys. J. **523**, 177 (1998).

[6] J. Granot, T. Piran, and R. Sari, Astron. & Astrophys. Suppl. Ser. **138**, 541 (1999).

[7] T. J. Galama et al. (1999), `astro-ph/9903021`.

[8] P. M. Vreeswijk et al., Astrophys. J. **523**, 171 (1999).

[9] K.-I. Nishikawa et al., Astrophys. J. **595**, 555 (2003).

[10] J. T. Frederiksen, C. B. Hededal, T. Haugbolle, and A. Nordlund (2003), `astro-ph/0303360`.

[11] J. T. Frederiksen, C. B. Hededal, T. Haugbolle, and A. Nordlund (2003), `astro-ph/0303360`.

[12] P. Yoon, Phys. Fluids B: Plasma Phys. **3**, 3074 (1991).

[13] F. Califano, F. Pegoraro, and S. V. Bulanov, Phys. Rev. E **56**, 963 (1997).

[14] P. Yoon and R. Davidson, Phys. Rev. A **35**, 2718 (1987).

[15] Y. Kazimura, J. Sakai, T. Neubert, and S. Bulanov, Astrophys. J. **498**, L183 (1998).

[16] F. Califano, T. Cecchi, and C. Chiuderi, Phys. Plasmas **9**, 451 (2002).

[17] R. Sari, R. Narayan, and T. Piran, Astrophys. J. **485**, 270 (1996).

[18] F. Califano, F. Pegoraro, S. V. Bulanov, and A. Mangeney, Phys. Rev. E **57**, 7048 (1998).